Electronic Supplementary Information

Revealing truncated conical geometry of nanochannels in anodic aluminium oxide membranes

Junxi Zhang,*[a], Huaping Zhao,[b] Ming Gong,[c] Lide Zhang,[d] Zhijun Yan,[e] Kang Xie,[f] Guangtao Fei,[d] Xiaoguang Zhu,[d] Mingguang Kong,[d] Shuyuan Zhang,[g] Lin Zhang [h] and Yong Lei,*[b]

[a] School of Instrument Science and Opto-electronics Engineering, Anhui Key Laboratory of Advanced Functional Materials and Devices, and Anhui Province Key Laboratory of Measuring Theory and Precision Instrument, Hefei University of Technology, Hefei 230009, China.

[b] Institute of Physics & IMN MacroNanos, Ilmenau University of Technology, Ilmenau 98693, Germany.

[c] Laboratory of Engineering and Material Science, University of Science and Technology of China, Hefei 230027, China.

[d] Key Laboratory of Materials Physics, Institute of Solid State Physics, Chinese Academy of Sciences, Hefei 230031, China.

[e] School of Optical and Electronic Information, Huazhong University of Science and Technology, Wuhan 430074, China.

[f] School of Opto-Electronic Engineering, Zaozhuang University, Zaozhuang 277160, Shandong, China.

[g] Hefei National Laboratory for Physical Sciences at Microscale, University of Science and Technology of China, Hefei 230026, China.

[h] Aston Institute of Photonic Technologies, School of Engineering & Applied Science, Aston University, Birmingham B4 7ET, UK.

*Email: junxi.zhang@hfut.edu.cn; yong.lei@tu-ilmenau.de

1. Measurements of optical reflection spectra of the cross sections of AAO membranes.

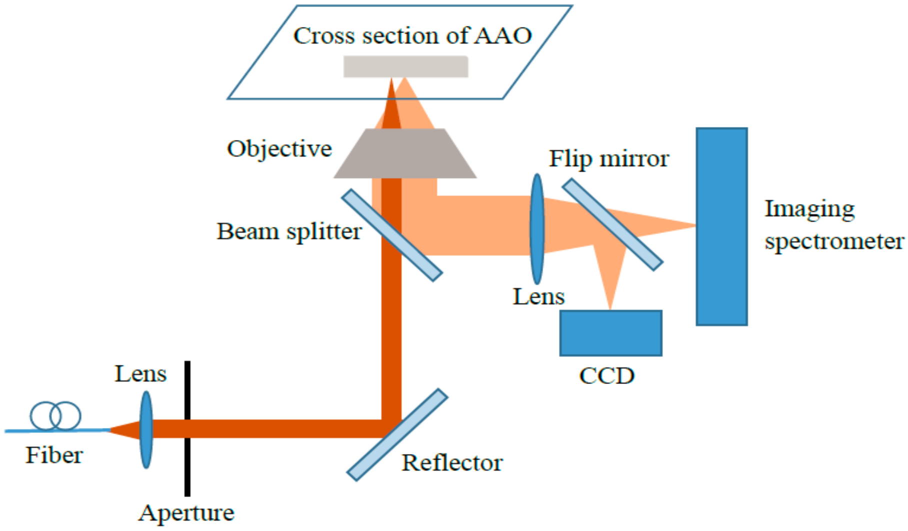

Fig. S1. Schematic illustration of micro-spectroscopy measurements of the cross sections of AAO membrane by a confocal microscope (Olympus, 100×) with an imaging spectrometer (iHR550).

2. Measurements of sizes and their distributions of the top and the bottom nanochannels of AAO membranes by a Gatan DigitalMicrograph (DM) software

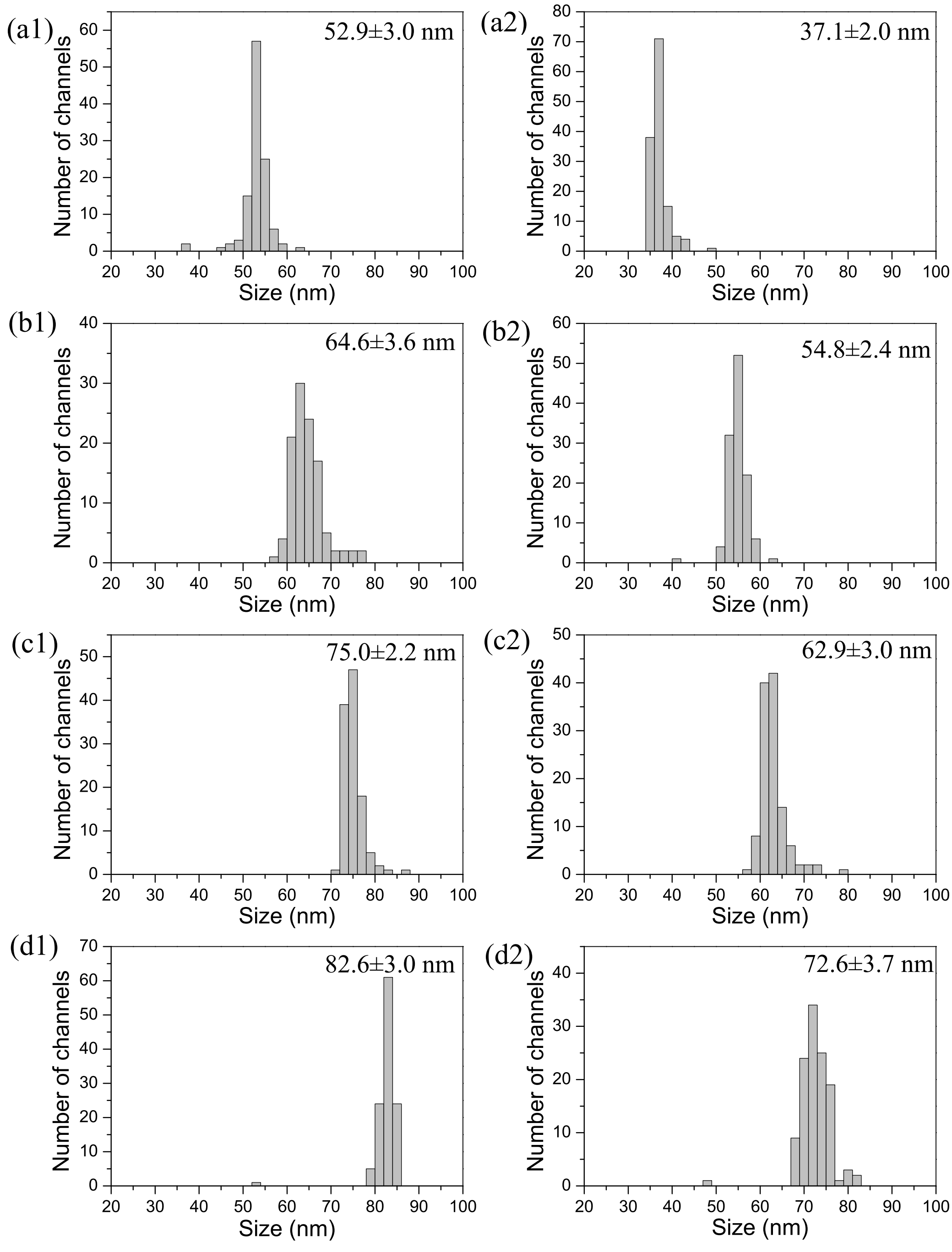

Fig. S2. Size distribution histograms of the top and the bottom nanochannels in the through-channel AAO membranes prepared at 13 ºC for 640 min. (a1), (b1), (c1) and (d1) show the size distributions of the top nanochannels in the AAO membranes after the etching for 0, 10, 35, and 60 min, respectively. (a2), (b2), (c2) and (d2) represent those of the bottom nanochannels in the same AAO membranes corresponding to (a1), (b1), (c1) and (d1), respectively.

(a)

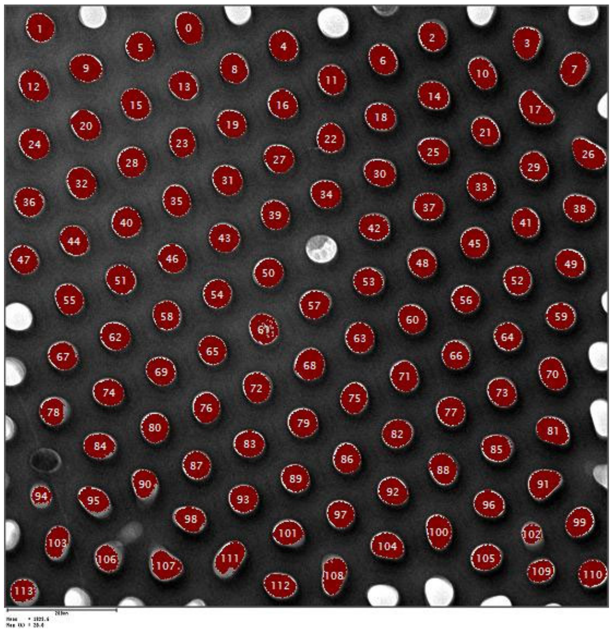

(b)

	FilledArea	CircDiamete
R0	2280.0	54.5703
R1	2202.0	52.8572
R2	2134.0	52.2179
R3	2312.0	54.6199
R4	2327.0	54.3323
R5	2203.0	52.7833
R6	2254.0	53.7435
R7	2377.0	56.3166
R8	2227.0	53.2053
R9	2422.0	55.6042
R10	2239.0	54.257
R11	2172.0	52.5
R12	2413.0	55.8402
R13	2185.0	52.8192
R14	2325.0	54.6116
R15	2379.0	55.3362
R16	2267.0	53.5268
R17	2678.0	62.209
R18	2211.0	53.1303
R19	2145.0	52.0844
R20	2380.0	55.1158
R21	2090.0	51.7755
R22	2139.0	52.0692
R23	2057.0	51.0926
R24	2479.0	56.1755
R25	2229.0	53.4065
R26	2560.0	59.2971
R27	2233.0	53.088
R28	2332.0	54.1737
R29	2207.0	52.876
R30	2282.0	54.0926
R31	2380.0	54.8145
R32	2470.0	56.2757
R33	2101.0	51.4682
R34	2238.0	53.2642
R35	2310.0	54.26
R36	2284.0	53.7183
R37	2238.0	53.3121

	FilledArea	CircDiamete
R38	2356.0	55.0827
R39	2216.0	52.8828
R40	2397.0	54.9763
R41	2118.0	51.6865
R42	2157.0	52.5234
R43	2336.0	54.3882
R44	2284.0	54.0327
R45	2237.0	53.159
R46	2180.0	52.4772
R47	2137.0	52.0755
R48	2157.0	52.5649
R49	2191.0	52.7649
R50	2223.0	53.0789
R51	2323.0	54.2185
R52	2135.0	51.9912
R53	2185.0	52.6043
R54	2167.0	52.3258
R55	2302.0	54.2594
R56	2040.0	50.6056
R57	2276.0	53.64
R58	2184.0	52.6598
R59	2053.0	50.9348
R60	2189.0	52.5032
R61	2347.0	54.5372
R62	2236.0	53.1033
R63	2279.0	53.6277
R64	2064.0	50.9652
R65	2160.0	52.1235
R66	2125.0	51.7783
R67	2179.0	52.5587
R68	2492.0	56.3321
R69	2210.0	52.7655
R70	2320.0	54.9786
R71	2237.0	53.3981
R72	2238.0	53.314
R73	2183.0	52.7069
R74	2192.0	52.7517
R75	2218.0	53.1606

	FilledArea	CircDiamete
R76	2219.0	53.1239
R77	2225.0	53.0537
R78	1841.0	48.8374
R79	2275.0	53.5428
R80	2179.0	52.4814
R81	2344.0	55.6951
R82	2249.0	53.3933
R83	2189.0	52.6894
R84	2132.0	52.5734
R85	2181.0	52.6339
R86	2172.0	52.3992
R87	2081.0	51.2947
R88	2258.0	53.8119
R89	2084.0	51.2297
R90	1882.0	49.6917
R91	2400.0	56.842
R92	2179.0	52.6142
R93	2167.0	52.3374
R94	1047.0	37.6003
R95	2022.0	52.3591
R96	2200.0	52.8532
R97	1990.0	49.9813
R98	2104.0	52.5097
R99	2157.0	52.417
R100	2266.0	54.6898
R101	1994.0	50.6999
R102	1091.0	37.665
R103	1944.0	51.8077
R104	2281.0	54.6635
R105	2111.0	51.8812
R106	1650.0	46.2372
R107	2308.0	55.9856
R108	2360.0	58.2672
R109	1612.0	45.4601
R110	2068.0	51.122
R111	2371.0	57.8847
R112	2144.0	52.9468
R113	1626.0	47.0765

Fig. S2-a1. (a) TEM image of the top surface of the AAO membrane without the chemical etching corresponding the analyzed nanochannels after the thresholding based on the DM software, the thresholding is the process of separating the top surfaces of the nanochannels from the rest of the image. (b) Measurements of the sizes (diameter, unit: nm) of the analyzed nanochannels on the top surface of the AAO membrane.

(a)

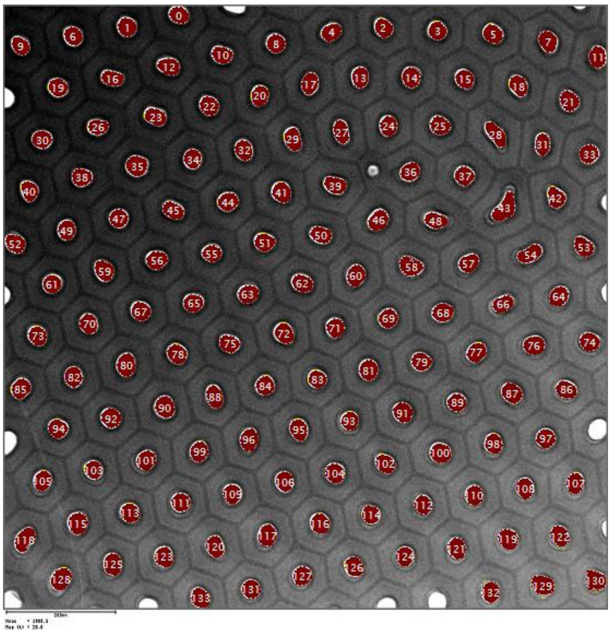

(b)

	FilledArea	CircDiamete
R0	969.0	35.1442
R1	1028.0	35.8529
R2	973.0	35.2076
R3	966.0	34.8069
R4	969.0	35.357
R5	1071.0	36.8437
R6	999.0	35.5366
R7	1104.0	37.6434
R8	997.0	35.3292
R9	901.0	34.0675
R10	1019.0	36.3045
R11	1059.0	36.9223
R12	1073.0	37.5598
R13	995.0	35.6727
R14	1050.0	36.5989
R15	1002.0	35.6701
R16	973.0	36.189
R17	1029.0	36.5219
R18	1055.0	37.1527
R19	1008.0	35.6667
R20	996.0	35.6642
R21	1100.0	37.44
R22	1022.0	35.803
R23	1087.0	37.8755
R24	975.0	35.1048
R25	1049.0	36.4966
R26	899.0	34.466
R27	1051.0	38.0627
R28	1161.0	42.4691
R29	1116.0	38.865
R30	1008.0	35.6095
R31	965.0	35.9241
R32	1035.0	36.2293
R33	1047.0	36.2545
R34	990.0	35.2827
R35	1268.0	40.1151
R36	1016.0	35.9082
R37	1064.0	36.7211
R38	1013.0	35.8891
R39	1092.0	38.0244
R40	983.0	35.7382
R41	1111.0	37.4741
R42	1051.0	37.2357
R43	1507.0	49.4749
R44	1081.0	36.8168

	FilledArea	CircDiamete
R45	1023.0	36.6071
R46	1184.0	38.9227
R47	987.0	35.1543
R48	1073.0	37.9379
R49	981.0	35.265
R50	1039.0	36.7843
R51	1051.0	36.5621
R52	1034.0	36.4569
R53	1056.0	37.1339
R54	1143.0	40.7469
R55	919.0	34.0752
R56	1098.0	37.424
R57	1022.0	36.338
R58	1236.0	40.4201
R59	1090.0	37.4675
R60	1112.0	37.6477
R61	986.0	35.2608
R62	1068.0	36.9094
R63	1054.0	36.4824
R64	1061.0	36.7523
R65	1019.0	35.9233
R66	980.0	36.1629
R67	1047.0	36.3408
R68	1117.0	37.6377
R69	1039.0	36.2255
R70	1014.0	35.7761
R71	987.0	35.1349
R72	1142.0	37.9424
R73	1017.0	35.7787
R74	1069.0	36.7916
R75	1010.0	35.9045
R76	1141.0	38.0043
R77	1073.0	36.8321
R78	1101.0	37.328
R79	1053.0	36.4441
R80	1228.0	39.761
R81	1116.0	37.4504
R82	1038.0	36.2519
R83	951.0	34.493
R84	1038.0	36.098
R85	1086.0	37.0931
R86	1077.0	37.1516
R87	1171.0	38.767
R88	1072.0	37.7382
R89	992.0	35.2596

	FilledArea	CircDiamete
R90	1237.0	39.7094
R91	1109.0	37.2961
R92	1102.0	37.1813
R93	938.0	34.1619
R94	1050.0	36.4048
R95	1091.0	37.388
R96	1119.0	38.0326
R97	1052.0	36.3877
R98	1024.0	36.1348
R99	1037.0	36.15
R100	1206.0	38.9986
R101	1068.0	36.7029
R102	1047.0	36.6739
R103	976.0	34.9363
R104	1112.0	37.4179
R105	1037.0	36.1443
R106	1054.0	36.5915
R107	1059.0	36.9477
R108	1038.0	36.4689
R109	1057.0	36.4231
R110	1037.0	36.1691
R111	1038.0	36.0716
R112	968.0	35.0199
R113	1066.0	36.6012
R114	976.0	35.1715
R115	1223.0	39.36
R116	1132.0	37.7858
R117	1143.0	38.086
R118	1260.0	42.0887
R119	1197.0	39.1042
R120	1113.0	37.9974
R121	1085.0	37.2107
R122	1101.0	40.0643
R123	1104.0	37.3577
R124	1007.0	35.6787
R125	1138.0	38.2325
R126	1075.0	36.9632
R127	1057.0	36.5514
R128	1292.0	41.1262
R129	1358.0	43.9933
R130	1302.0	42.7455
R131	1004.0	35.6434
R132	1152.0	39.9754
R133	1083.0	37.1432

Fig. S2-a2. (a) TEM image of the bottom surface of the AAO membrane without the chemical etching corresponding the analyzed nanochannels after the thresholding. (b) Measurements of the sizes (diameter, unit: nm) of the analyzed nanochannels on the bottom surface of the AAO membrane.

(a)

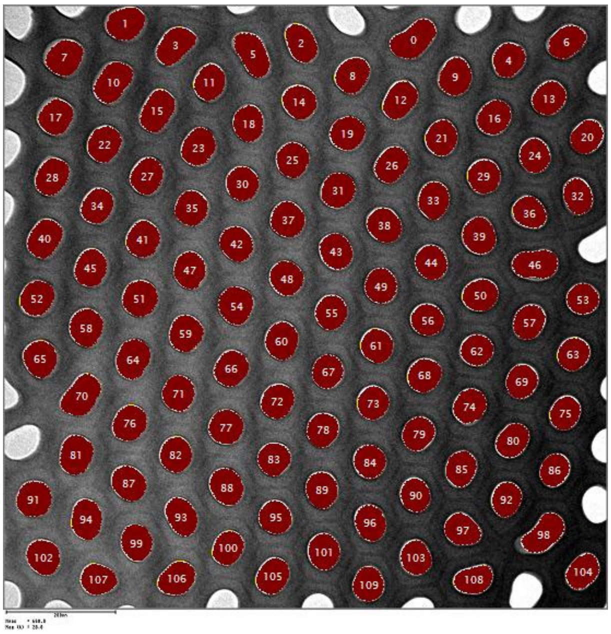

(b)

	FilledArea	CircDiamete
R0	4167.0	77.6757
R1	3498.0	67.4905
R2	3268.0	66.457
R3	3630.0	71.5134
R4	3028.0	62.229
R5	3881.0	75.6831
R6	3218.0	65.6902
R7	3600.0	68.6301
R8	3345.0	66.147
R9	3381.0	66.1198
R10	3911.0	73.4747
R11	3087.0	63.1614
R12	3445.0	67.6725
R13	3071.0	62.6109
R14	3193.0	63.9643
R15	3749.0	71.588
R16	3121.0	63.217
R17	3365.0	66.195
R18	3031.0	63.0992
R19	3211.0	64.1397
R20	2925.0	61.1658
R21	3121.0	63.076
R22	3294.0	65.2193
R23	3435.0	66.6708
R24	2877.0	60.49
R25	3125.0	63.3171
R26	3190.0	64.4361
R27	3235.0	64.7648
R28	3402.0	67.0302
R29	3052.0	62.223
R30	3062.0	62.6399
R31	3259.0	64.5252
R32	2834.0	60.7193
R33	3150.0	63.8152
R34	3129.0	63.809
R35	3160.0	63.9215
R36	2927.0	61.442

	FilledArea	CircDiamete
R37	3308.0	64.9664
R38	3244.0	64.3283
R39	3360.0	65.6243
R40	3521.0	68.4586
R41	3376.0	66.0066
R42	3184.0	63.8943
R43	3242.0	64.4
R44	3067.0	62.3407
R45	3332.0	65.7603
R46	3731.0	72.1334
R47	3271.0	65.3114
R48	3173.0	63.5631
R49	3104.0	62.7311
R50	3152.0	63.3401
R51	3479.0	66.4856
R52	3266.0	65.0981
R53	2706.0	58.4801
R54	3567.0	67.607
R55	3023.0	62.1885
R56	2902.0	60.5846
R57	2993.0	61.8261
R58	3442.0	66.7767
R59	3375.0	66.3239
R60	3415.0	66.0713
R61	3029.0	61.9671
R62	2808.0	59.5754
R63	2883.0	60.4642
R64	3673.0	69.6643
R65	3373.0	65.8686
R66	3359.0	65.6857
R67	2856.0	60.241
R68	3082.0	62.5579
R69	2913.0	60.9172
R70	4087.0	76.1574
R71	3191.0	64.1867
R72	3129.0	63.1673
R73	2925.0	60.8457

	FilledArea	CircDiamete
R74	3102.0	63.2596
R75	2781.0	59.6734
R76	3347.0	65.8187
R77	3285.0	64.8512
R78	2983.0	61.7607
R79	2984.0	61.6382
R80	3005.0	62.3286
R81	3631.0	69.1948
R82	3154.0	63.618
R83	2962.0	61.2668
R84	2923.0	60.7592
R85	2987.0	61.9611
R86	2619.0	57.9694
R87	3310.0	65.2305
R88	3394.0	66.1628
R89	3196.0	64.0321
R90	2775.0	59.4063
R91	3518.0	67.0897
R92	2820.0	60.1941
R93	3267.0	65.9851
R94	3489.0	68.1474
R95	3008.0	61.7714
R96	3032.0	62.4314
R97	3087.0	63.647
R98	3836.0	75.2311
R99	3167.0	63.9809
R100	2916.0	61.401
R101	3153.0	63.3854
R102	3294.0	65.3829
R103	2920.0	61.1132
R104	3029.0	63.2184
R105	3247.0	64.6985
R106	3359.0	66.5047
R107	3085.0	63.2313
R108	3053.0	64.3793
R109	2924.0	61.0265

Fig. S2-b1. (a) TEM image of the top surface of the AAO membrane with the chemical etching for 10 min corresponding the analyzed nanochannels after the thresholding. (b) Measurements of the sizes (diameter, unit: nm) of the analyzed nanochannels on the top surface of the AAO membranes.

(a)

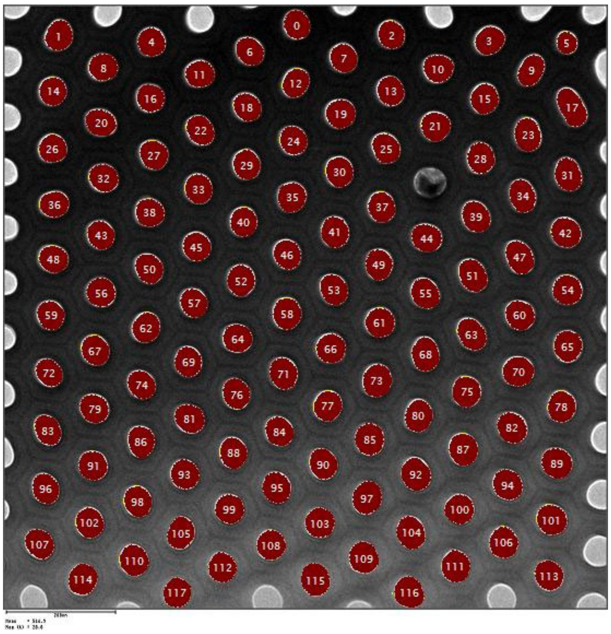

(b)

	FilledArea	CircDiamete
R0	2079.0	51.2939
R1	2313.0	54.3009
R2	2103.0	51.579
R3	2345.0	54.5909
R4	2201.0	52.6374
R5	1310.0	40.6007
R6	2126.0	52.0292
R7	2181.0	52.6036
R8	2174.0	52.4641
R9	2192.0	53.7233
R10	2340.0	54.5578
R11	2178.0	52.5422
R12	2162.0	52.4098
R13	2207.0	52.9048
R14	2162.0	52.15
R15	2328.0	54.2432
R16	2151.0	52.2516
R17	2843.0	63.2774
R18	2162.0	52.3407
R19	2368.0	54.6665
R20	2251.0	53.7247
R21	2379.0	54.877
R22	2262.0	53.8521
R23	2463.0	56.3214
R24	2164.0	52.265
R25	2322.0	54.4543
R26	2215.0	52.8736
R27	2294.0	53.9513
R28	2371.0	54.8696
R29	2264.0	53.6002
R30	2329.0	54.3841
R31	2431.0	56.0737
R32	2259.0	53.381
R33	2282.0	53.6814
R34	2383.0	55.6423
R35	2335.0	54.3869
R36	2119.0	51.8547
R37	2308.0	54.0974
R38	2266.0	53.5994
R39	2417.0	55.5691

	FilledArea	CircDiamete
R40	2199.0	52.6575
R41	2405.0	55.2177
R42	2481.0	56.0682
R43	2162.0	52.2697
R44	2335.0	54.3686
R45	2244.0	53.2282
R46	2264.0	53.6645
R47	2534.0	57.625
R48	2202.0	52.8003
R49	2292.0	54.0297
R50	2277.0	53.8563
R51	2523.0	57.3226
R52	2419.0	55.3442
R53	2302.0	54.2118
R54	2423.0	55.2956
R55	2393.0	55.2973
R56	2325.0	54.0728
R57	2167.0	52.3082
R58	2515.0	56.4181
R59	2195.0	52.6626
R60	2386.0	54.9368
R61	2413.0	55.2032
R62	2336.0	54.4041
R63	2509.0	57.1509
R64	2321.0	54.2183
R65	2473.0	56.0713
R66	2415.0	55.1542
R67	2337.0	54.3995
R68	2607.0	58.0236
R69	2275.0	53.6458
R70	2580.0	57.1253
R71	2431.0	55.6644
R72	2022.0	50.8936
R73	2637.0	57.8636
R74	2173.0	52.497
R75	2457.0	55.7355
R76	2299.0	54.0809
R77	2402.0	55.0423
R78	2465.0	55.9482
R79	2307.0	54.1034

	FilledArea	CircDiamete
R80	2491.0	56.4411
R81	2363.0	54.8216
R82	2540.0	56.8558
R83	2209.0	53.5119
R84	2302.0	54.0322
R85	2579.0	57.1011
R86	2359.0	54.9194
R87	2629.0	57.7226
R88	2378.0	54.9124
R89	2564.0	56.9075
R90	2401.0	55.2779
R91	2344.0	54.3236
R92	2693.0	58.6762
R93	2367.0	54.6353
R94	2525.0	56.6326
R95	2448.0	55.7301
R96	2260.0	53.7248
R97	2669.0	58.3209
R98	2410.0	55.3911
R99	2384.0	54.8803
R100	2434.0	55.4636
R101	2577.0	57.2283
R102	2395.0	55.0361
R103	2451.0	55.6854
R104	2610.0	57.771
R105	2426.0	55.9656
R106	2520.0	56.5984
R107	2343.0	54.6553
R108	2437.0	55.4899
R109	2638.0	58.0958
R110	2532.0	56.6683
R111	2581.0	57.3283
R112	2371.0	55.1474
R113	2407.0	55.3354
R114	2552.0	57.0706
R115	2702.0	59.8972
R116	2618.0	58.3722
R117	2341.0	55.4722

Fig. S2-b2. (a) TEM image of the bottom surface of the AAO membrane with the chemical etching for 10 min corresponding the analyzed nanochannels after the thresholding. (b) Measurements of the sizes (diameter, unit: nm) of the analyzed nanochannels on the bottom surface of the AAO membrane.

(a)

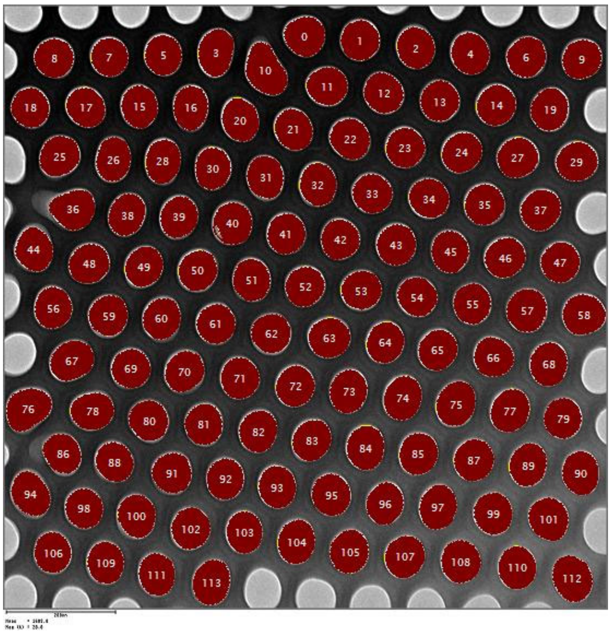

(b)

	FilledArea	CircDiamete
R0	4436.0	75.0419
R1	4305.0	73.8115
R2	4334.0	74.2148
R3	4620.0	78.1811
R4	4375.0	74.635
R5	4148.0	72.5747
R6	4306.0	73.9202
R7	3965.0	70.7805
R8	4199.0	72.8204
R9	4241.0	73.2941
R10	5493.0	87.4851
R11	4308.0	73.8878
R12	4351.0	74.2685
R13	4311.0	73.8504
R14	4385.0	74.4691
R15	4232.0	73.5419
R16	4263.0	74.3756
R17	4231.0	73.284
R18	4106.0	72.1669
R19	4409.0	75.0037
R20	4396.0	75.1272
R21	4276.0	73.8147
R22	4431.0	75.0577
R23	4263.0	73.4885
R24	4393.0	74.7402
R25	4470.0	75.5554
R26	4245.0	74.1824
R27	4520.0	75.641
R28	4303.0	74.6337
R29	4478.0	75.2952
R30	4192.0	73.1995
R31	4319.0	74.3011
R32	4358.0	74.5772
R33	4268.0	73.449
R34	4317.0	73.8885
R35	4465.0	75.2224
R36	4856.0	80.2167
R37	4523.0	75.7924

	FilledArea	CircDiamete
R38	4222.0	73.6575
R39	4268.0	73.8445
R40	4568.0	76.0984
R41	4245.0	73.2745
R42	4237.0	73.2824
R43	4455.0	75.1267
R44	4487.0	76.1703
R45	4313.0	74.0724
R46	4468.0	75.2709
R47	4298.0	73.7585
R48	4387.0	74.5602
R49	4177.0	72.9285
R50	4368.0	74.591
R51	4339.0	74.465
R52	4306.0	73.8482
R53	4315.0	73.96
R54	4255.0	73.3879
R55	4176.0	72.7508
R56	4275.0	73.783
R57	4723.0	77.4459
R58	4819.0	78.3528
R59	4354.0	74.504
R60	4289.0	74.023
R61	4208.0	72.9745
R62	4259.0	73.7248
R63	4604.0	76.421
R64	4294.0	73.8242
R65	4378.0	74.5994
R66	4348.0	74.2547
R67	4739.0	78.0809
R68	4518.0	76.0376
R69	4178.0	72.6368
R70	4378.0	74.9031
R71	4385.0	74.5639
R72	4397.0	74.6471
R73	4485.0	75.7311
R74	4645.0	77.1648
R75	4832.0	78.884

	FilledArea	CircDiamete
R76	5159.0	82.4848
R77	4644.0	77.0534
R78	4473.0	75.5718
R79	4209.0	73.099
R80	4347.0	74.2592
R81	4269.0	73.779
R82	4394.0	74.8334
R83	4418.0	74.9646
R84	4636.0	77.0618
R85	4532.0	75.8982
R86	4089.0	72.7373
R87	4602.0	76.4336
R88	4132.0	72.4152
R89	4453.0	75.6278
R90	4453.0	75.8099
R91	4391.0	74.6935
R92	4242.0	73.4376
R93	4409.0	75.0307
R94	4648.0	78.1886
R95	4485.0	75.4773
R96	4327.0	74.2688
R97	4570.0	76.6463
R98	4124.0	72.359
R99	4508.0	75.8343
R100	4501.0	76.0066
R101	4695.0	77.394
R102	4456.0	75.1711
R103	4224.0	73.4156
R104	4579.0	76.7955
R105	4663.0	77.1009
R106	4174.0	72.9151
R107	4649.0	76.9123
R108	4674.0	77.0009
R109	4282.0	74.0181
R110	4532.0	76.1444
R111	4253.0	73.7926
R112	5042.0	80.9738
R113	4664.0	77.5866

Fig. S2-c1. (a) TEM image of the top surface of the AAO membrane with the chemical etching for 35 min corresponding the analyzed nanochannels after the thresholding. (b) Measurements of the sizes (diameter, unit: nm) of the analyzed nanochannels on the top surface of the AAO membranes.

(a)

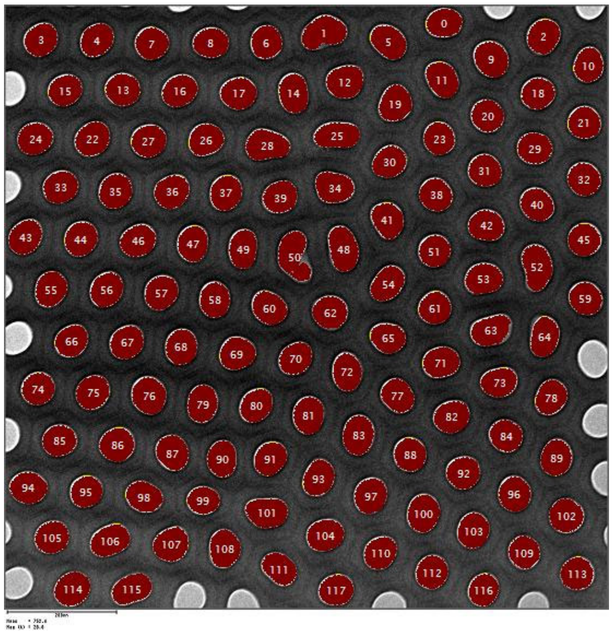

(b)

	FilledArea	CircDiamete
R0	2878.0	60.8983
R1	3800.0	73.368
R2	3071.0	62.5195
R3	2981.0	61.6469
R4	2922.0	61.1829
R5	3214.0	64.7874
R6	2841.0	59.9673
R7	2944.0	60.9583
R8	2902.0	60.9081
R9	3345.0	65.2976
R10	2797.0	59.8655
R11	3111.0	63.594
R12	3320.0	65.2738
R13	3058.0	62.2073
R14	3226.0	65.1062
R15	2860.0	60.2729
R16	3065.0	62.7506
R17	3141.0	63.1788
R18	2874.0	60.3391
R19	3228.0	64.4757
R20	2849.0	59.9866
R21	2896.0	60.5291
R22	3207.0	64.1001
R23	2790.0	59.3751
R24	3054.0	62.3643
R25	3339.0	69.3243
R26	3043.0	62.422
R27	3084.0	62.5632
R28	3664.0	70.8198
R29	2973.0	61.4729
R30	2937.0	61.2704
R31	2895.0	60.5612
R32	2957.0	61.1248
R33	3054.0	62.3653
R34	3326.0	66.2659
R35	3113.0	62.767
R36	3160.0	63.5541
R37	3065.0	62.4828
R38	2927.0	60.9277
R39	2995.0	61.7181
R40	2967.0	61.5634
R41	3092.0	63.2992
R42	3018.0	62.0976
R43	3086.0	63.0298
R44	3091.0	62.6624
R45	2934.0	60.8575
R46	3101.0	62.992
R47	3025.0	62.2724
R48	3628.0	70.7519
R49	3004.0	63.0533
R50	3973.0	78.9509
R51	2761.0	59.0271
R52	3675.0	72.1167
R53	3182.0	64.2085
R54	3037.0	63.4268
R55	3022.0	62.2313
R56	3085.0	62.712
R57	3061.0	62.3631
R58	2942.0	61.3279
R59	2929.0	60.9198
R60	3095.0	63.1882
R61	2850.0	60.0808
R62	3105.0	62.8122
R63	3282.0	67.4711
R64	3125.0	64.6425
R65	2864.0	60.5996
R66	2850.0	60.2786
R67	3014.0	61.9234
R68	3059.0	62.4256
R69	3153.0	63.4917
R70	2865.0	60.6087
R71	3133.0	63.3999
R72	3006.0	62.6052
R73	2933.0	61.6794
R74	2914.0	60.7499
R75	3049.0	62.2421
R76	3502.0	66.7628
R77	2944.0	61.5647
R78	2962.0	61.6738
R79	3114.0	63.4715
R80	2951.0	61.6084
R81	3095.0	63.2044
R82	3103.0	62.9415
R83	3380.0	66.0598
R84	2872.0	60.2722
R85	2913.0	60.8116
R86	3217.0	63.8821
R87	3117.0	63.0734
R88	2968.0	61.2021
R89	3040.0	62.37
R90	2899.0	61.1985
R91	2939.0	61.2386
R92	2962.0	61.253
R93	3079.0	63.1341
R94	3227.0	64.233
R95	2778.0	59.2874
R96	3033.0	61.9734
R97	3172.0	63.5383
R98	3046.0	62.7583
R99	2494.0	56.2443
R100	3325.0	65.3786
R101	3464.0	68.1431
R102	3154.0	63.1806
R103	3062.0	62.5112
R104	3223.0	64.4534
R105	3033.0	62.1281
R106	3364.0	66.7943
R107	3295.0	64.9908
R108	3224.0	64.6849
R109	2794.0	59.4979
R110	2899.0	60.836
R111	2893.0	61.732
R112	2949.0	61.0776
R113	2977.0	61.3371
R114	3307.0	64.9373
R115	3252.0	66.4147
R116	2700.0	58.5719
R117	2953.0	61.4475

Fig. S2-c2. (a) TEM image of the bottom surface of the AAO membrane with the chemical etching for 35 min corresponding the analyzed nanochannels after the thresholding. (b) Measurements of the sizes (diameter, unit: nm) of the analyzed nanochannels on the bottom surface of the AAO membrane.

(a)

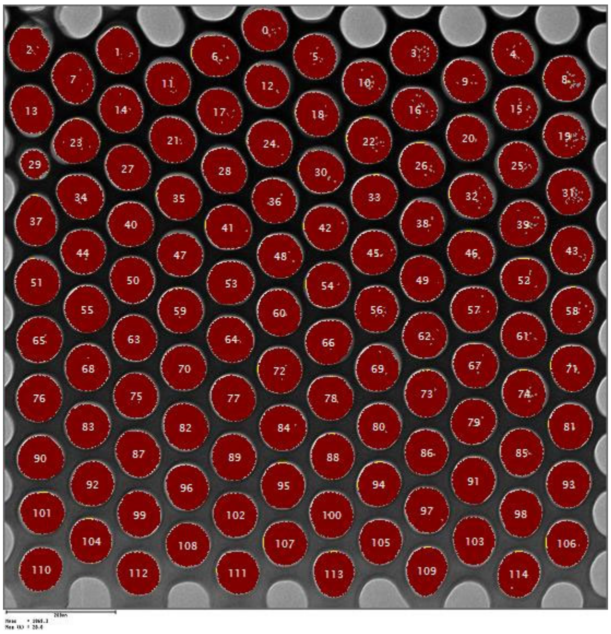

(b)

	FilledArea	CircDiamete
R0	5164.0	81.3076
R1	5190.0	81.5911
R2	4797.0	79.1318
R3	5598.0	84.2104
R4	5023.0	80.3729
R5	5145.0	80.9501
R6	5479.0	83.9666
R7	5486.0	84.5675
R8	5136.0	81.1881
R9	4945.0	79.5335
R10	5320.0	82.3126
R11	5262.0	82.0333
R12	5153.0	81.5302
R13	5417.0	84.1189
R14	5349.0	82.5674
R15	4981.0	79.6637
R16	5341.0	82.4525
R17	5433.0	83.1568
R18	5245.0	81.7281
R19	4999.0	79.9145
R20	5099.0	80.945
R21	5657.0	84.9728
R22	5561.0	84.0533
R23	5451.0	83.4536
R24	5588.0	84.4297
R25	4987.0	79.9528
R26	5368.0	82.9008
R27	5407.0	83.0974
R28	5448.0	83.5516
R29	2189.0	53.3376
R30	5297.0	82.2954
R31	5319.0	82.2438
R32	5169.0	81.4144
R33	5522.0	83.6236
R34	5532.0	84.2442
R35	5440.0	83.3723
R36	5339.0	82.4565
R37	5478.0	84.6049
R38	5254.0	82.0216

	FilledArea	CircDiamete
R39	5604.0	84.384
R40	5427.0	82.9761
R41	5551.0	83.9997
R42	5265.0	81.8817
R43	5390.0	82.9505
R44	5306.0	82.061
R45	5330.0	82.2311
R46	5562.0	84.0964
R47	5282.0	81.9485
R48	5295.0	82.0327
R49	5454.0	83.2543
R50	5481.0	83.5308
R51	5610.0	84.534
R52	5450.0	83.2479
R53	5521.0	83.7778
R54	5349.0	82.465
R55	5593.0	84.2676
R56	5368.0	82.6404
R57	5632.0	84.7561
R58	5458.0	83.4161
R59	5490.0	83.4725
R60	5499.0	83.6823
R61	5439.0	83.0819
R62	5462.0	83.2946
R63	5405.0	82.9261
R64	5677.0	85.0142
R65	5536.0	83.7704
R66	5567.0	84.2145
R67	5484.0	83.5169
R68	5590.0	84.2554
R69	5415.0	83.1036
R70	5480.0	83.3843
R71	5459.0	83.4139
R72	5465.0	83.2398
R73	5508.0	83.7613
R74	5591.0	84.3519
R75	5378.0	82.663
R76	5671.0	84.8092
R77	5560.0	84.0689

	FilledArea	CircDiamete
R78	5392.0	82.792
R79	5483.0	83.4755
R80	5400.0	82.9098
R81	5436.0	83.1403
R82	5642.0	84.7981
R83	5398.0	82.967
R84	5702.0	85.0459
R85	5518.0	83.8685
R86	5275.0	81.9675
R87	5483.0	83.811
R88	5408.0	82.7909
R89	5552.0	84.029
R90	5546.0	84.0274
R91	5495.0	83.6185
R92	5250.0	81.7522
R93	5468.0	83.4888
R94	5297.0	82.022
R95	5466.0	83.3232
R96	5322.0	82.4596
R97	5365.0	82.6228
R98	5371.0	82.8105
R99	5364.0	82.58
R100	5489.0	83.6192
R101	5123.0	80.8299
R102	5323.0	82.2692
R103	5489.0	84.0531
R104	5172.0	81.1133
R105	5228.0	81.5523
R106	5258.0	81.9099
R107	5296.0	81.9956
R108	5227.0	81.4489
R109	5334.0	83.2071
R110	5120.0	80.8192
R111	5056.0	80.2532
R112	5143.0	80.9187
R113	5116.0	81.0385
R114	5263.0	81.903

Fig. S2-d1. (a) TEM image of the top surface of the AAO membrane with the chemical etching for 60 min corresponding the analyzed nanochannels after the thresholding. (b) Measurements of the sizes (diameter, unit: nm) of the analyzed nanochannels on the top surface of the AAO membrane.

(a)

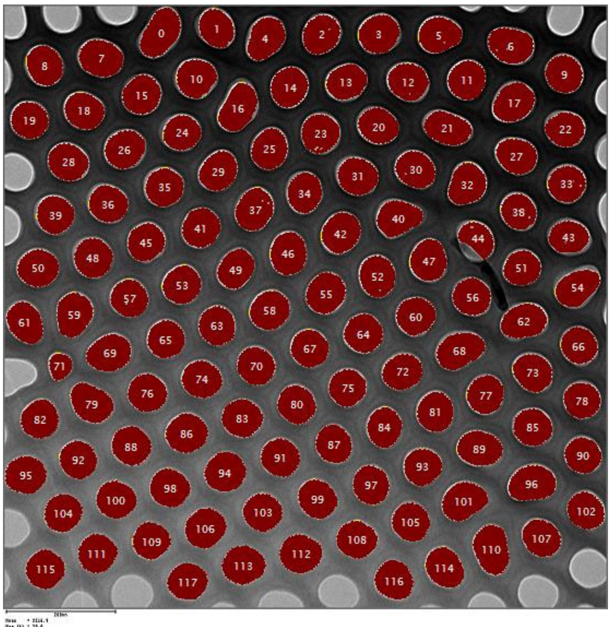

(b)

	FilledArea	CircDiamete
R0	4925.0	82.9708
R1	3767.0	69.4588
R2	4044.0	71.884
R3	4341.0	74.3388
R4	4280.0	75.7398
R5	4205.0	73.9961
R6	4483.0	76.7119
R7	4514.0	76.2178
R8	4001.0	71.4952
R9	3863.0	69.908
R10	4276.0	74.1223
R11	4068.0	71.8126
R12	4176.0	73.0008
R13	3997.0	71.5954
R14	4152.0	72.5951
R15	4118.0	72.3579
R16	4725.0	81.0487
R17	4397.0	75.524
R18	4043.0	71.803
R19	3815.0	69.4566
R20	3961.0	71.0614
R21	4275.0	76.3001
R22	3710.0	68.8924
R23	4108.0	72.3695
R24	3687.0	68.4515
R25	4055.0	72.0059
R26	4203.0	73.4156
R27	4048.0	72.2553
R28	4199.0	73.1195
R29	4100.0	72.6159
R30	4015.0	71.6691
R31	4167.0	73.0086
R32	4362.0	75.4902
R33	3845.0	69.883
R34	3871.0	70.6035
R35	4059.0	71.8989
R36	3993.0	71.4225
R37	4386.0	75.1341
R38	3544.0	67.1801
R39	3952.0	70.8573
R40	4359.0	76.9223
R41	4093.0	72.0994
R42	4350.0	74.5443
R43	3613.0	68.3328
R44	3158.0	67.3926
R45	3907.0	70.5791
R46	4345.0	74.595
R47	4238.0	73.6776
R48	4209.0	73.2779
R49	3887.0	70.9235
R50	4238.0	73.3324
R51	3588.0	67.4849
R52	4163.0	72.977
R53	4060.0	71.7301
R54	4244.0	76.2616
R55	4421.0	74.9259
R56	3914.0	70.4056
R57	3886.0	70.2241
R58	4306.0	73.9191
R59	4440.0	76.3253
R60	4063.0	71.8987
R61	4068.0	73.0575
R62	4411.0	76.7216
R63	3950.0	70.9213
R64	4113.0	72.2885
R65	3901.0	70.3256
R66	3705.0	68.5379
R67	3922.0	70.4532
R68	4676.0	79.7873
R69	4524.0	76.783
R70	3970.0	71.045
R71	1772.0	47.9722
R72	3946.0	70.9616
R73	4114.0	72.6501
R74	4121.0	72.3623
R75	3861.0	69.9345
R76	4084.0	71.9785
R77	3943.0	70.8099
R78	3657.0	68.1078
R79	4466.0	76.9699
R80	3996.0	71.3063
R81	4064.0	71.9966
R82	4045.0	71.8055
R83	4238.0	73.4956
R84	3838.0	70.1307
R85	4007.0	71.3948
R86	4524.0	75.762
R87	3828.0	69.8811
R88	4212.0	73.2766
R89	4410.0	75.7436
R90	3634.0	67.8122
R91	4068.0	71.8835
R92	3936.0	70.8565
R93	3921.0	70.7032
R94	4477.0	75.523
R95	4298.0	74.214
R96	4760.0	79.6593
R97	3914.0	70.62
R98	4234.0	73.5587
R99	4158.0	72.943
R100	4184.0	73.3069
R101	4635.0	78.302
R102	3804.0	69.6962
R103	4060.0	71.9818
R104	3985.0	71.3824
R105	3989.0	71.25
R106	4468.0	75.7798
R107	3928.0	70.9637
R108	4197.0	73.2216
R109	3853.0	70.6044
R110	4835.0	80.9928
R111	4131.0	72.9881
R112	4523.0	76.1875
R113	4591.0	76.955
R114	4233.0	74.2212
R115	4171.0	73.2254
R116	4165.0	73.1977
R117	4129.0	73.0797

Fig. S2-d2. (a) TEM image of the bottom surface of the AAO membrane with the chemical etching for 60 min corresponding the analyzed nanochannels after the thresholding. (b) Measurements of the sizes (diameter, unit: nm) of the analyzed nanochannels on the bottom surface of the AAO membrane.

3. Selected area electron diffraction patterns of the AAO membranes with different nanochannel sizes after partially covering the central transmitted beam by a beam stopper.

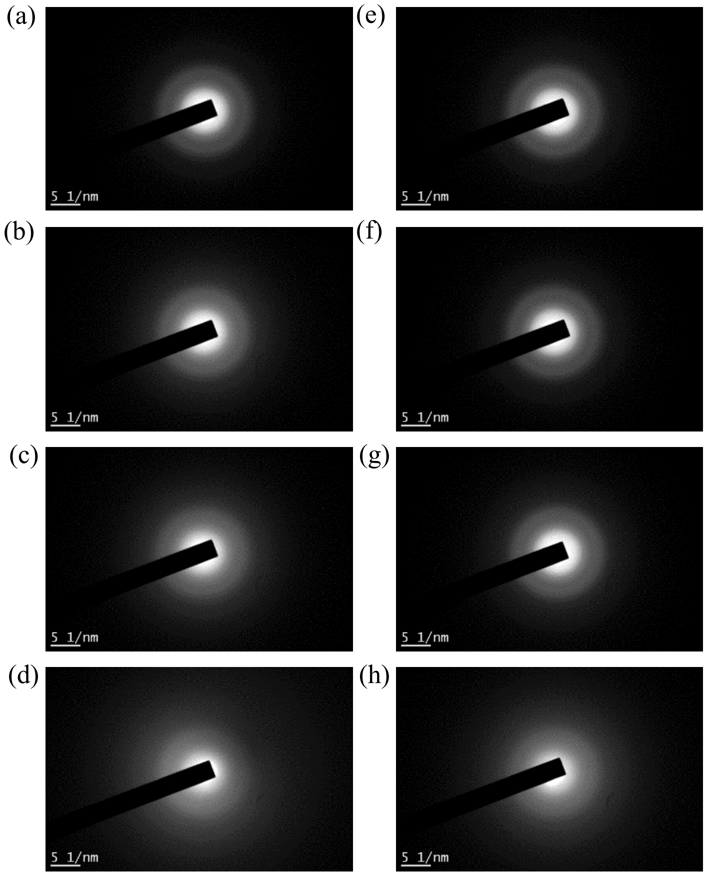

Fig. S3 Selected area electron diffraction patterns of the AAO membranes with different nanochannel sizes after partially covering the central transmitted beam by a beam stopper. (a), (b), (c) and (d) Top surfaces of the nanochannels in the AAO membranes formed after etching the through-channel membranes immersed in a 5 % H_3PO_4 solution at 30 °C for 0, 10, 35 and 60 min, respectively, corresponding to the nanochannel sizes of 52.9±3.0, 64.6±3.6, 75.0±2.2 and 82.6±3.0 nm. (e), (f), (g) and (h) Bottom surfaces of the nanochannels in the same membranes formed after etching the through-channel membranes for 0, 10, 35, and 60 min, respectively, corresponding to the nanochannel sizes of 37.1±2.0, 54.8±2.4, 62.9±3.0 and 72.6±3.7 nm.

4. Statistic measurements of 300 nanochannel spacings and theirs distributions on the top and the bottom surfaces for every AAO membrane by the DM software

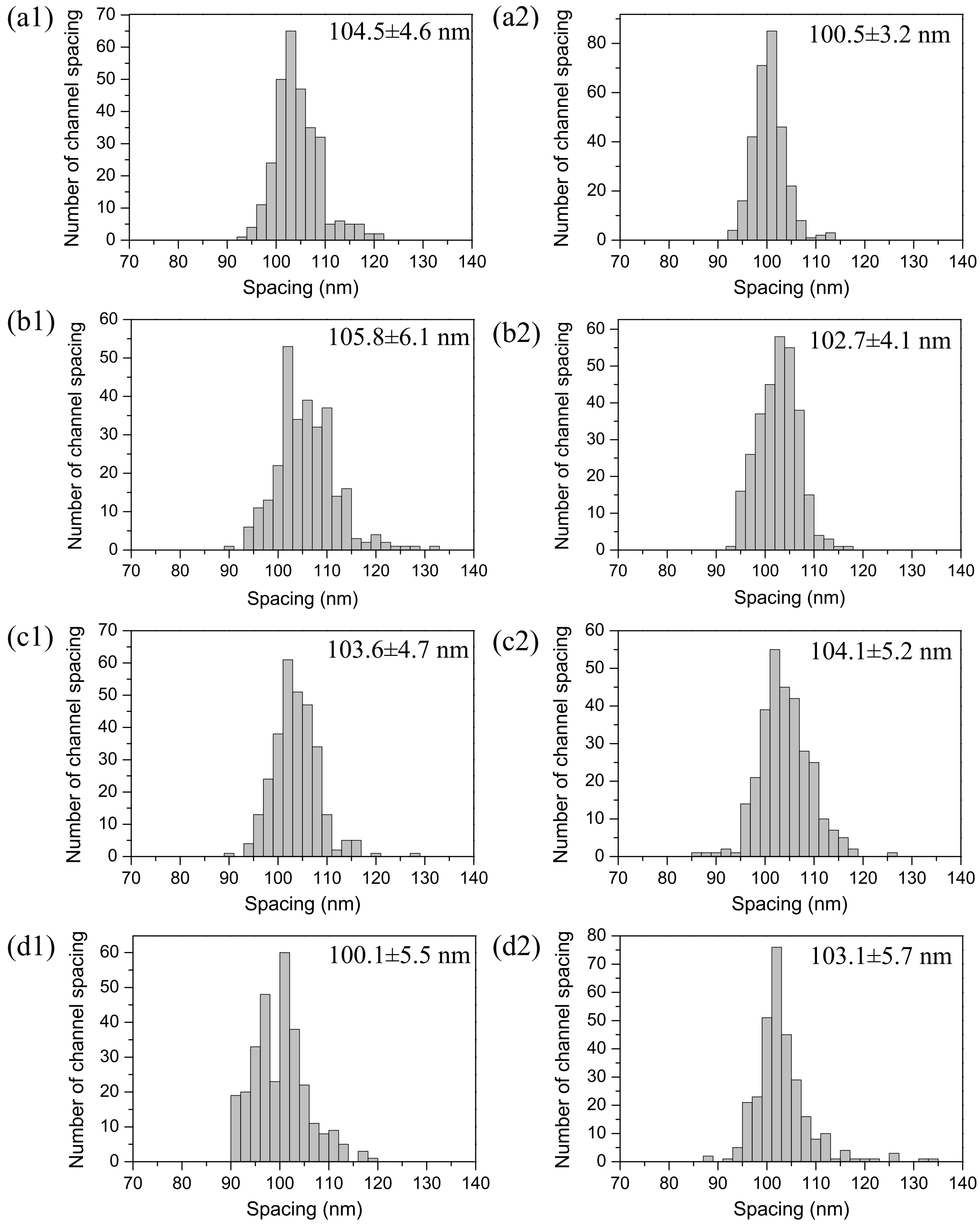

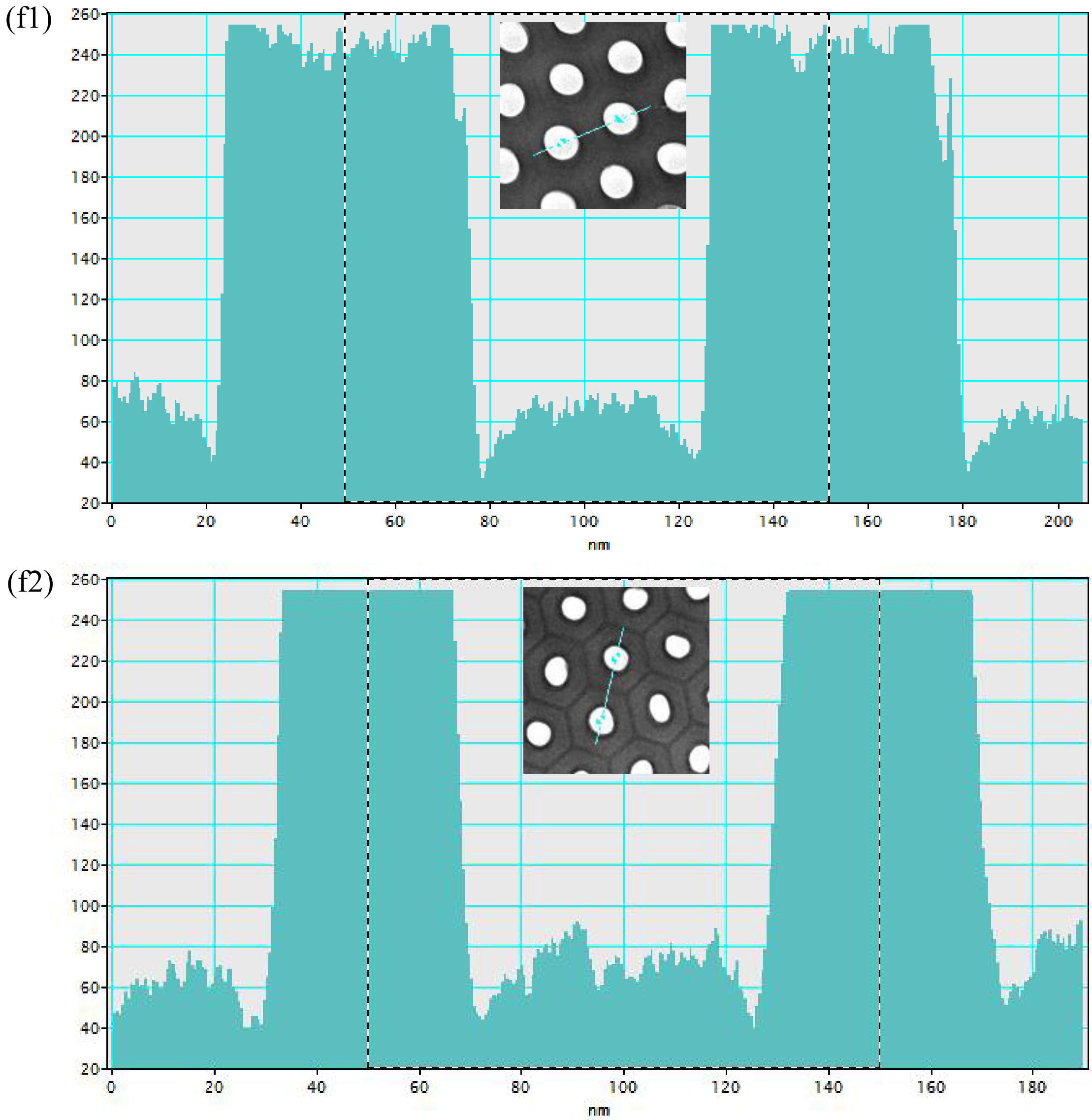

Fig. S4. Histograms of 300 nanochannel spacing on the top and bottom surfaces for every AAO membrane. (a1), (b1), (c1), and (d1) show the spacing distributions on the top surface of the membranes after the chemical etching for 0, 10, 35, and 60 min, respectively. (a2), (b2), (c2), and (d2) correspond to those on the bottom surfaces in the same membranes, respectively. (f1) and (f2) demonstrate the line profiles from one of two adjacent nanochannels by the DM software, respectively, the widths of the dashed-line frames represent the spacing of two adjacent nanochannels, insets: typical images of the spacing measurements based on the line profiles.

5. Reflection spectra of the top and the bottom surfaces of the truncated conical nanochannels in the as-prepared AAO membrane

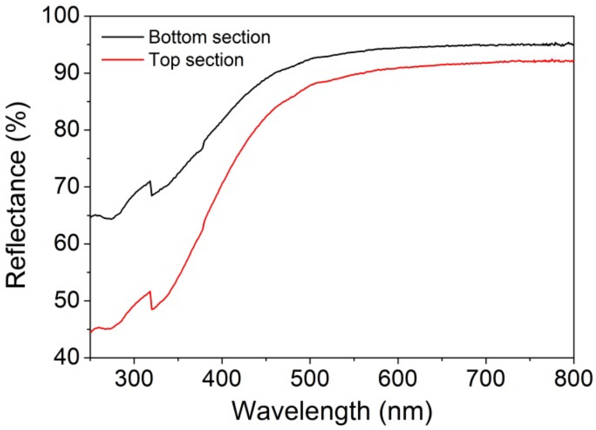

Fig. S5. Reflection spectra of the top and the bottom surfaces of the as-prepared 70 μm thick AAO membrane by using a UV-Vis-NIR spectrophotometer with an integrating sphere (PerkinElmer Lambda 750S).

6. Current density with anodization time at the self-ordering growth (steady-state) process

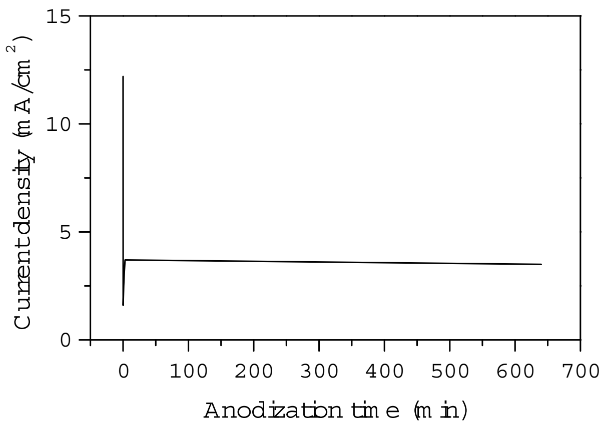

Fig. S6. Curve of the current density with the anodization time during the self-ordering growth of the AAO membranes (under the anodization voltage of 40 V at 13 °C).

7. Plot the experimental data of current density at different anodization temperatures

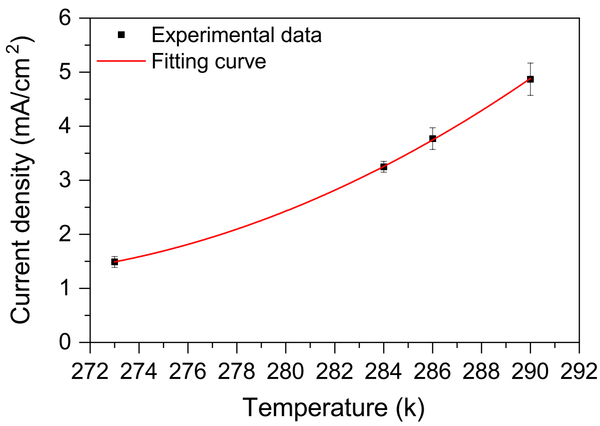

Fig. S7. Current density during the anodization process with the electrolyte temperature and the fit curve according the equation (3) in the text. The fitted results are $i_O = 1.45 \times 10^5$, $i_M = 1.00 \times 10^8$, $\alpha = 3300$, $\beta = 4800$.

8. Etching as-prepared through-channel AAO membranes based on the temperature gradient regime to achieve the nanochannels with cylindrical geometry

The as-prepared through-channel AAO membranes through a drying treatment were floated on the surface of a 5 % H_3PO_4 solution (Fig. S8), where the H_3PO_4 solution was put in a petri dish that was partially immersed into a digital-control water bath with a temperature of 30 °C by control of a heating element, the temperature of the bottom surface of the AAO membranes equals to that of the H_3PO_4 solution, which can be measured by a thermocouple fixed into the water bath. The digital-control water bath was put into a horizontal refrigerator with a surrounding temperature of 8 °C, the surrounding temperature can be controlled by the refrigerator, the temperature of the top surfaces of the AAO membrane exposed to the surrounding were measured by a mercury thermometer. The bottom surfaces of the membranes are in contact with the surface of the H_3PO_4 solution with a high temperature of 30 ºC by control of a constant temperature in a digital-control water bath, while the top surfaces are exposed to the surrounding with a low temperature of 8 ºC, this gives rise to a temperature gradient of the solution in the nanochannels from down to up based on a capillary phenomenon. In the case, the enlarging rate of the nanochannels on the bottom segment is larger than that on the top segment during the etching process, which results in the decrease of the original size deviation along the long axis of the nanochannels (Fig. 5a in the text). For the as-prepared through channel AAO membranes with different thicknesses (e.g., 27 μm, 60 μm, 70 μm and 93 μm), the etching time corresponds to 2 min, 5 min, 10 min and 40 min, respectively.

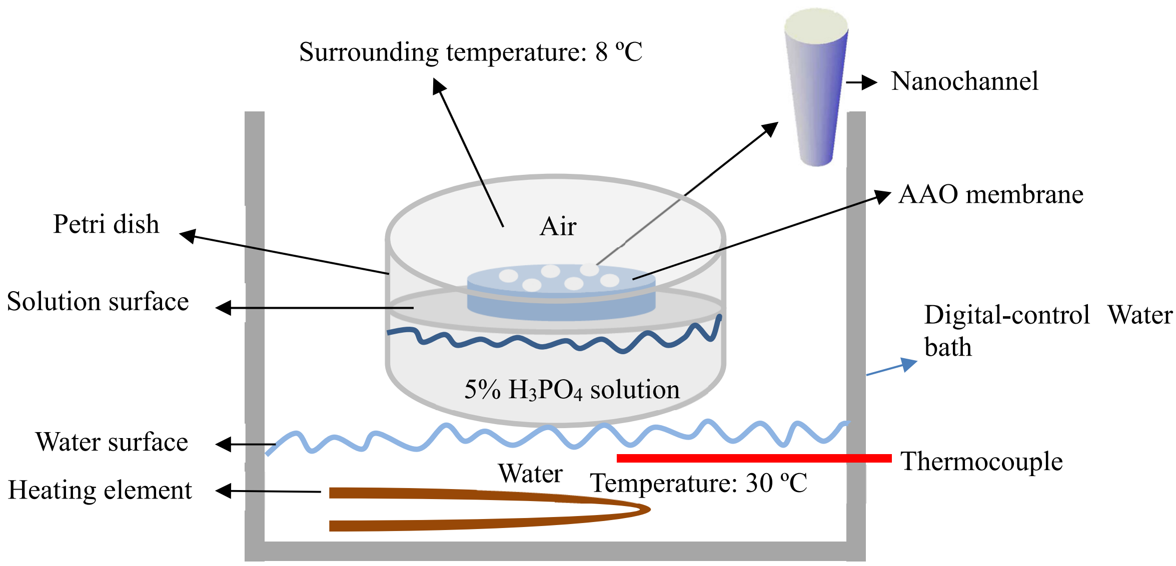

Fig. S8. Schematic illustration of the setup of the etching method based on the temperature gradient regime.

9. Morphologies and size distributions of the top and the bottom nanochannels in the through-channel AAO membranes formed at the constant voltage of 40 V and different electrolyte (anodization) temperatures

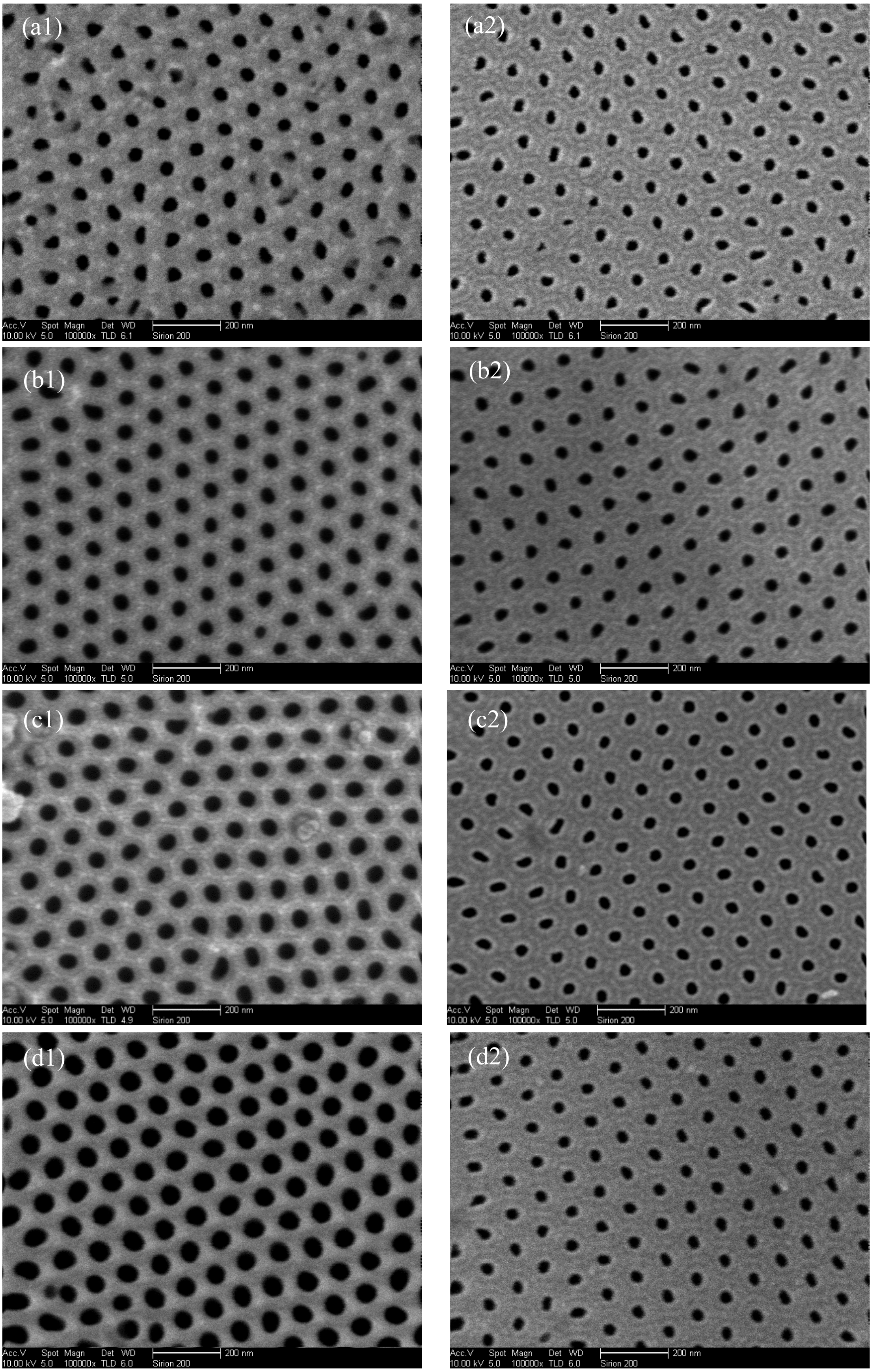

Fig. S9. SEM images of the top and bottom surfaces of the through-channel AAO membranes formed at the constant voltage of 40 V and different anodization temperatures, all of the through-channel membranes are not through any etching treatment. (a1), (a2) Top and bottom surfaces of a 27 μm thick membrane prepared through the second anodization at the constant temperature of 0°C for 660 min, respectively. (b1), (b2) Top and bottom surfaces of a 60 μm thick membrane prepared at 11°C for 720 min, respectively. (c1), (c2) Top and bottom surfaces of a 70 μm thick membrane prepared at 13°C for 640 min, respectively. (d1), (d2) Top and bottom surfaces of a 93 μm thick membrane prepared at 17°C for 660 min, respectively.

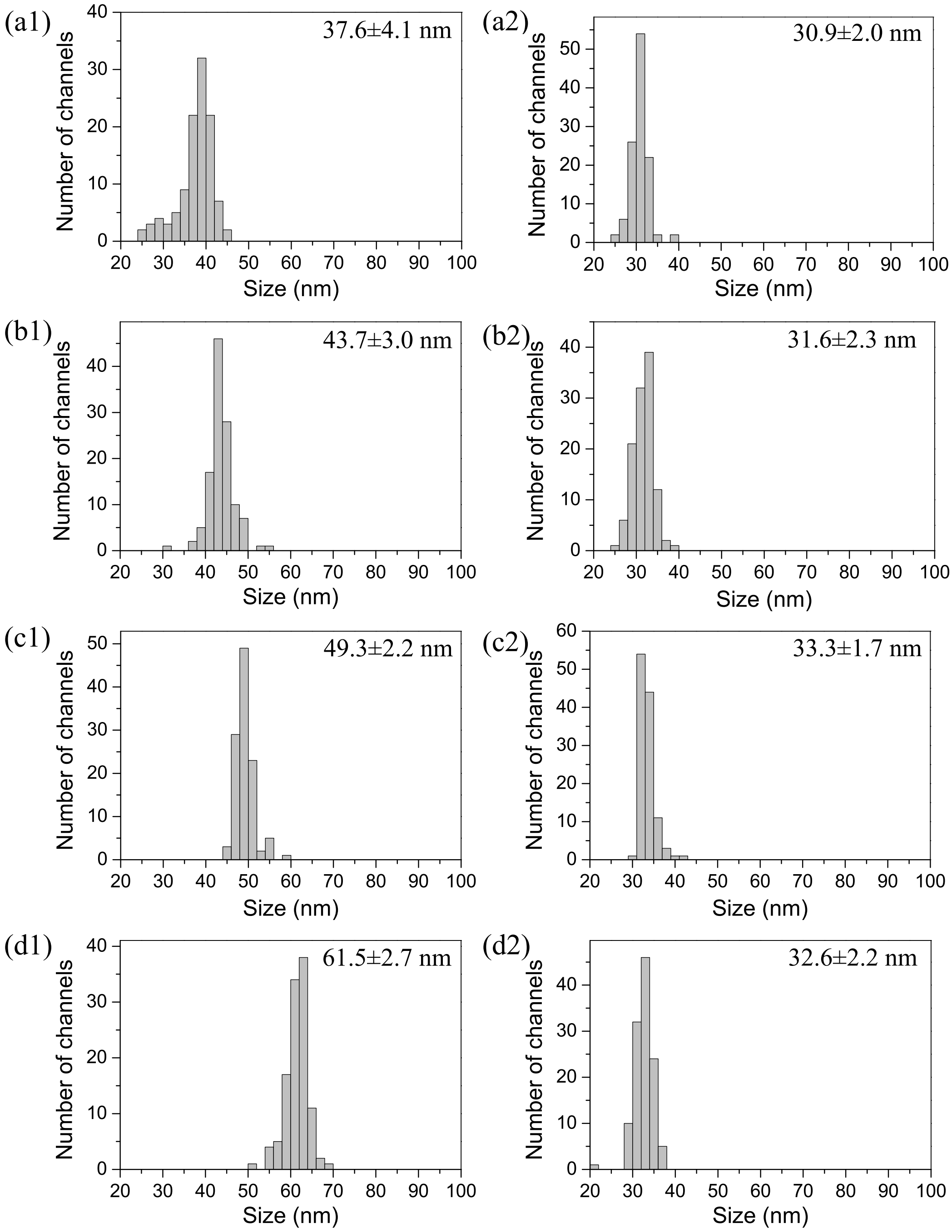

Fig. S10. Size distribution histograms of the top and bottom nanochannels in the corresponding through-channel AAO membranes shown in Fig. S9.

10. Reducing the size difference between the top and the bottom nanochannels in the AAO membranes by an effective etching method based on the temperature gradient regime

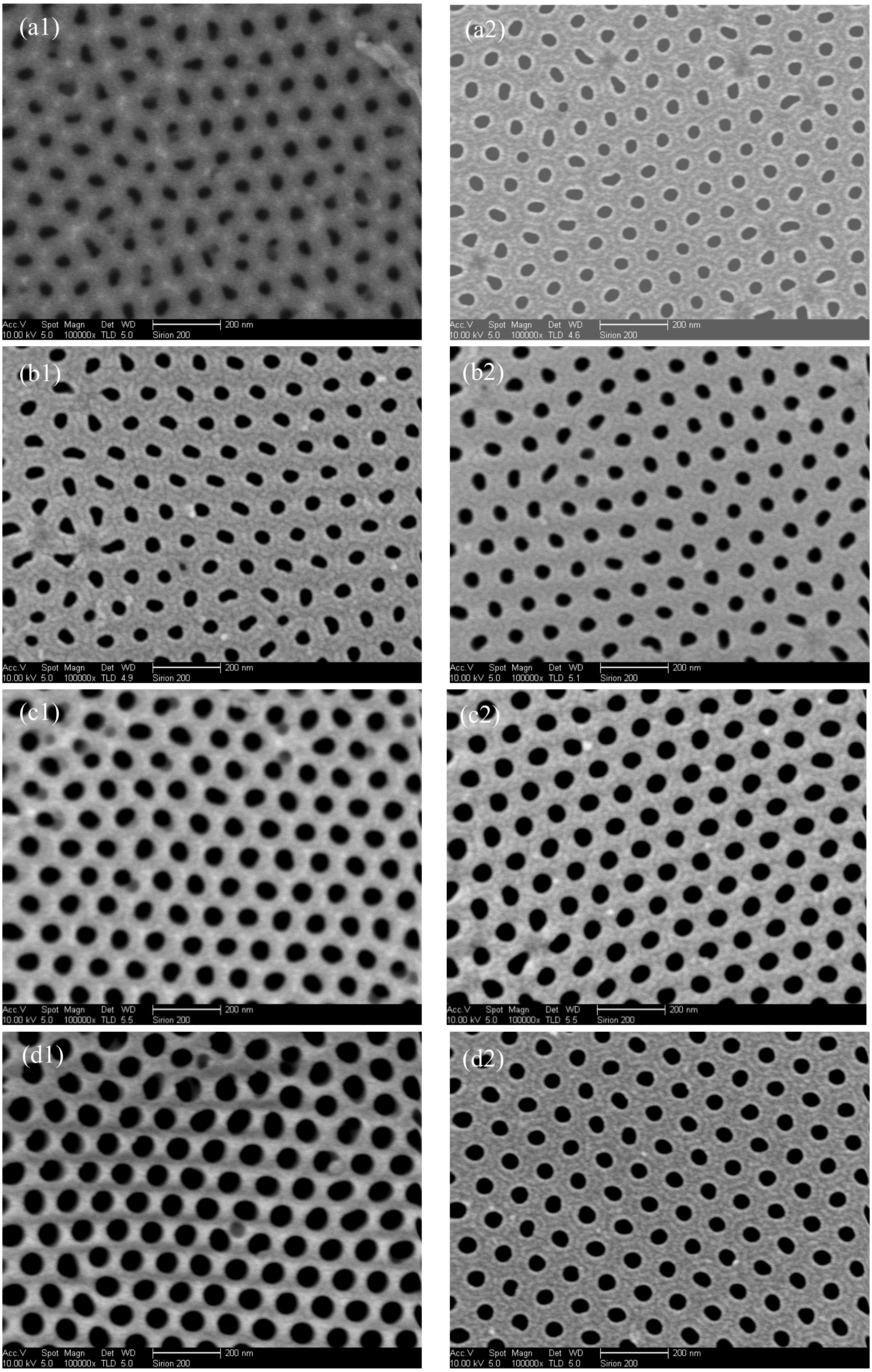

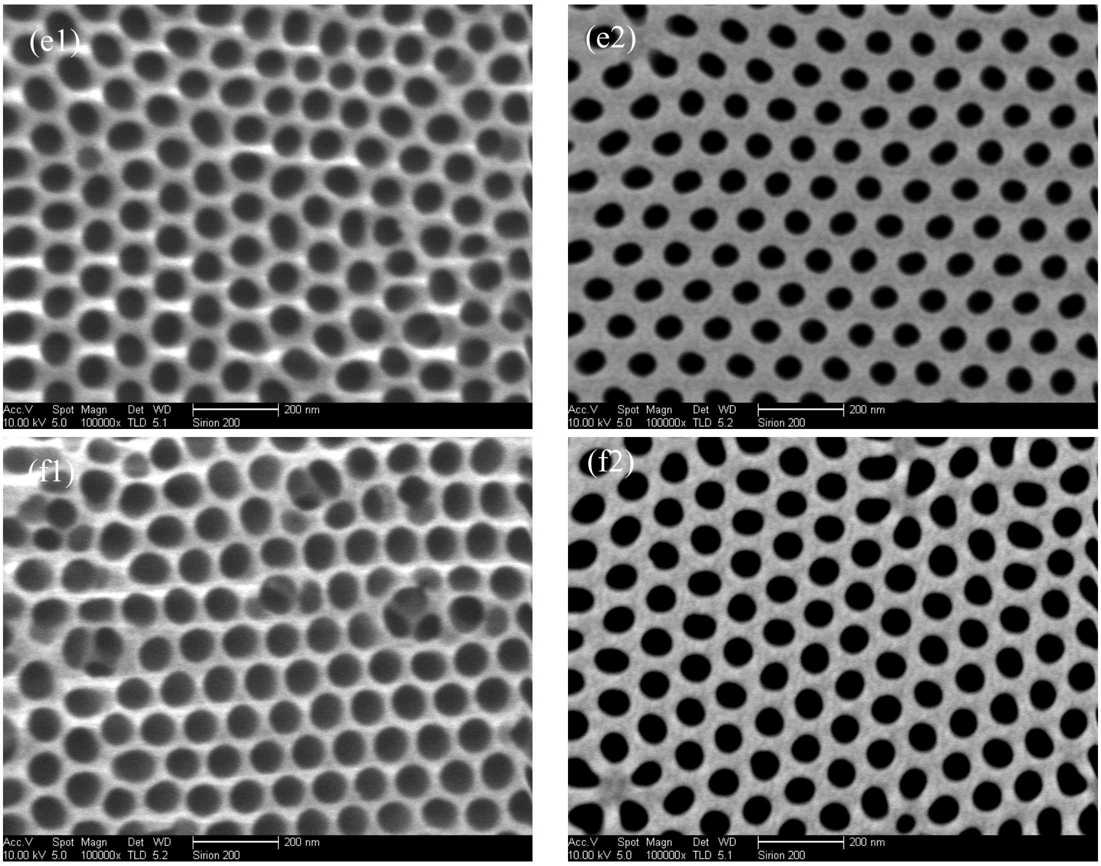

Fig. S11. SEM images of the top and the bottom surfaces of the AAO membranes by the etching method based on the temperature gradient regime. (a1), (a2) Top and bottom surfaces of the 27 μm thick membrane after the etching for 2 min, respectively. (b1), (b2) Top and bottom surfaces of the 60 μm thick membrane after the etching for 5 min, respectively. (c1), (c2) Top and bottom surfaces of the 70 μm thick membrane after the etching for 10 min, respectively. (d1)-(f1) Top surfaces of the 93 μm thick membranes after the etching for 10, 25, and 40 min, respectively, (d2)-(f2) Corresponding the bottom surfaces of the 93 μm thick membranes after the etching for 10, 25, and 40 min, respectively.

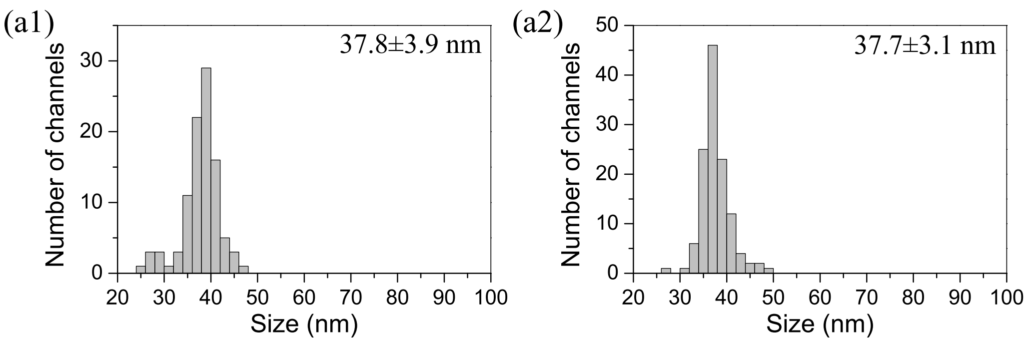

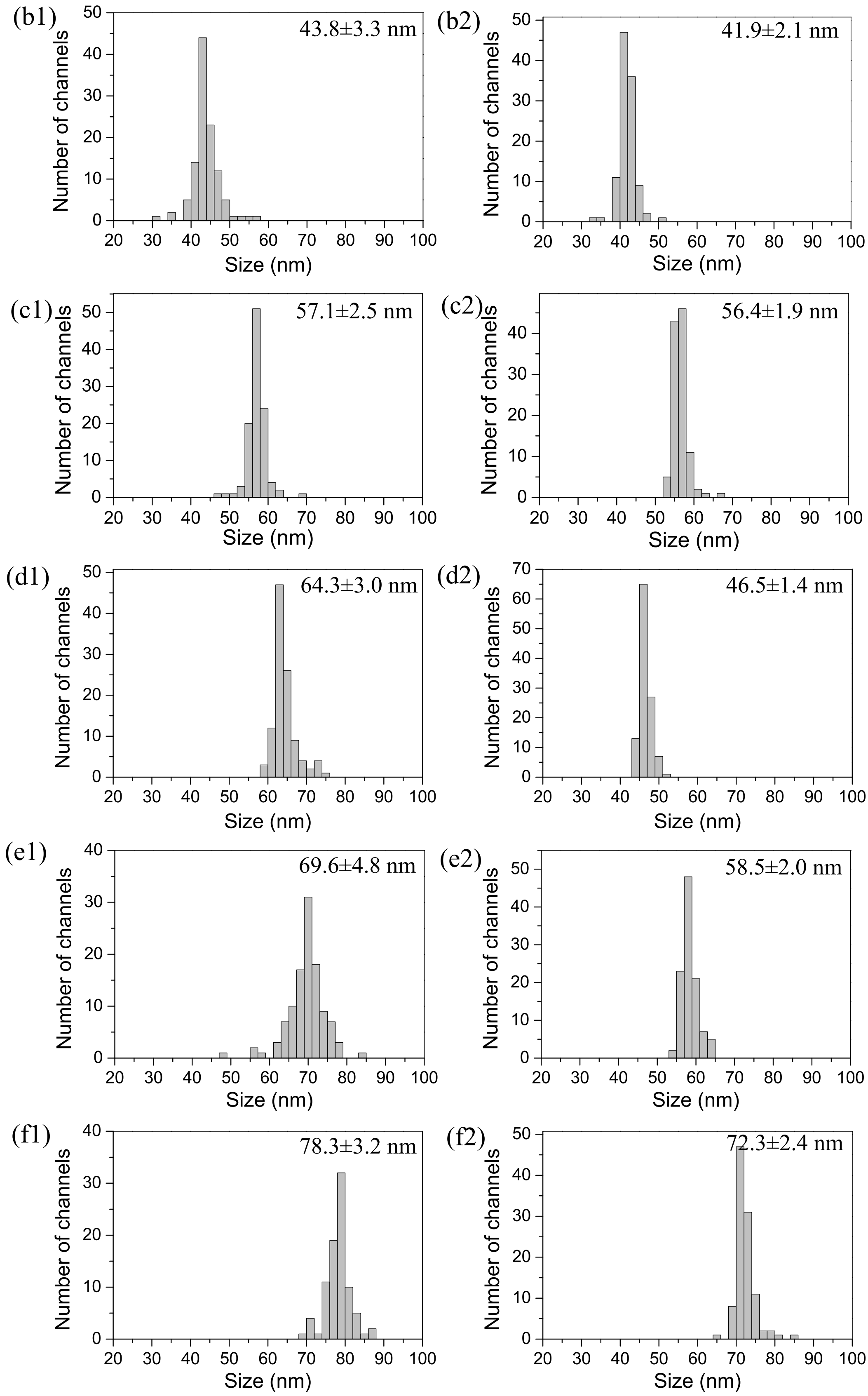

Fig. S12. Size distribution histograms of the top and the bottom nanochannels in the AAO membranes shown in Fig. S11.

11. Comparisons of the voltage compensation method, and constant anodization voltage and subsequent temperature gradient etching method to fabricate the AAO membranes

Consider the nanochannel size is linearly proportional to the anodization voltage during the anodization, Shang et al. proposed a voltage compensation method to fabricate the AAO membranes with uniform diameter of nanochannels (G. L. Shang et al. *Mater. Lett.* **110**, 156-159 (2013)). Note that the voltage compensation method presents the essentially different aspects when comparing our constant anodization voltage and subsequent temperature gradient etching method:

(a). Growth regimes of nanochannels in AAO membranes are entirely different

The growth regimes of the nanochannels in AAO membranes strongly depend on the anodization voltage. Furthermore, pore spacing, pore size and wall thickness are linearly proportional to the voltage during both mild anodization (MA) and hard anodization (HA) (W. Lee et al. *Nat. Mater.* **5,** 741-747 (2006)). In typical MA processes, self-ordered arrays of alumina nanopores can be obtained within three self-ordering growth regimes: (1) sulphuric acid at 25V for an interpore distance (D_{int})=63 nm, (2) oxalic acid at 40V for D_{int}=100 nm (W. Lee et al. *Nat. Mater.* **5,** 741-747 (2006)), and (3) phosphoric acid at 195V for D_{int}=500 nm, indicating the self-ordering growth regime represents the constant voltages during the anodization.

In our work, all of the AAO membranes were fabricated under the self-ordering regime: oxalic acid ($H_2C_2O_4$) at 40 V. The subsequent etching of the self-ordered AAO membranes only tune the nanochannel size but do not change their spacing and the ordered arrangement. That is, our AAO membranes fabricated under self-ordering regime and subsequent etching method are self-ordered nanochannel arrays.

In contrast, for the voltage compensation mode, the voltage was gradually increased from 40 to 52 V during the anodization. Obviously, the growth method has deviated from the self-ordering growth regime. As a result, the formed AAO membranes are not self-ordered nanochannel arrays (the detail will be given in (b)).

(b). Structures of the nanochannels in the AAO membranes fabricated by Shang's method and our method are extremely different due to the two completely different growth regimes

Firstly, in terms of the voltage compensation method

From the cross section SEM image (Fig. S13 from Shang's paper), it is found that the spacing between the nanochannels in the AAO membrane fabricated by the voltage compensation method, obviously increases along the long axis of the nanochannels from about 102 nm on the upper layer marked with U, to about 120 nm on the middle layer marked with M, and then to about 134 nm on the under layer marked with L, this is because the nanochannel spacing in the AAO membranes formed under ordinary MA conditions is linearly dependent on the voltage with a proportionality constant of 2.5 nmV^{-1} (W. Lee et al. *Nat. Mater.* **5,** 741-747 (2006), *Nat. Nanotechnol.* **3,** 234-239 (2008).) One can clearly observe that the spacing displays remarkable increase from up to down. Additionally, the nanochannel density deceases from up to down along the long axis. Since the nanochannel spacing continuously changes during the growth of the nanochannels from up to down with raising the anodization voltage gradually, the growth orientation is not coaxial, which results in a winding (not upright) growth of the nanochannels, especially the nanochannel structurers between the bottom and top sections are extremely different shown in the following surface SEM images, therefore, the nanochannel configuration is not cylindrical. That is, the cylindrical nanochannels cannot be fabricated by Shang's method.

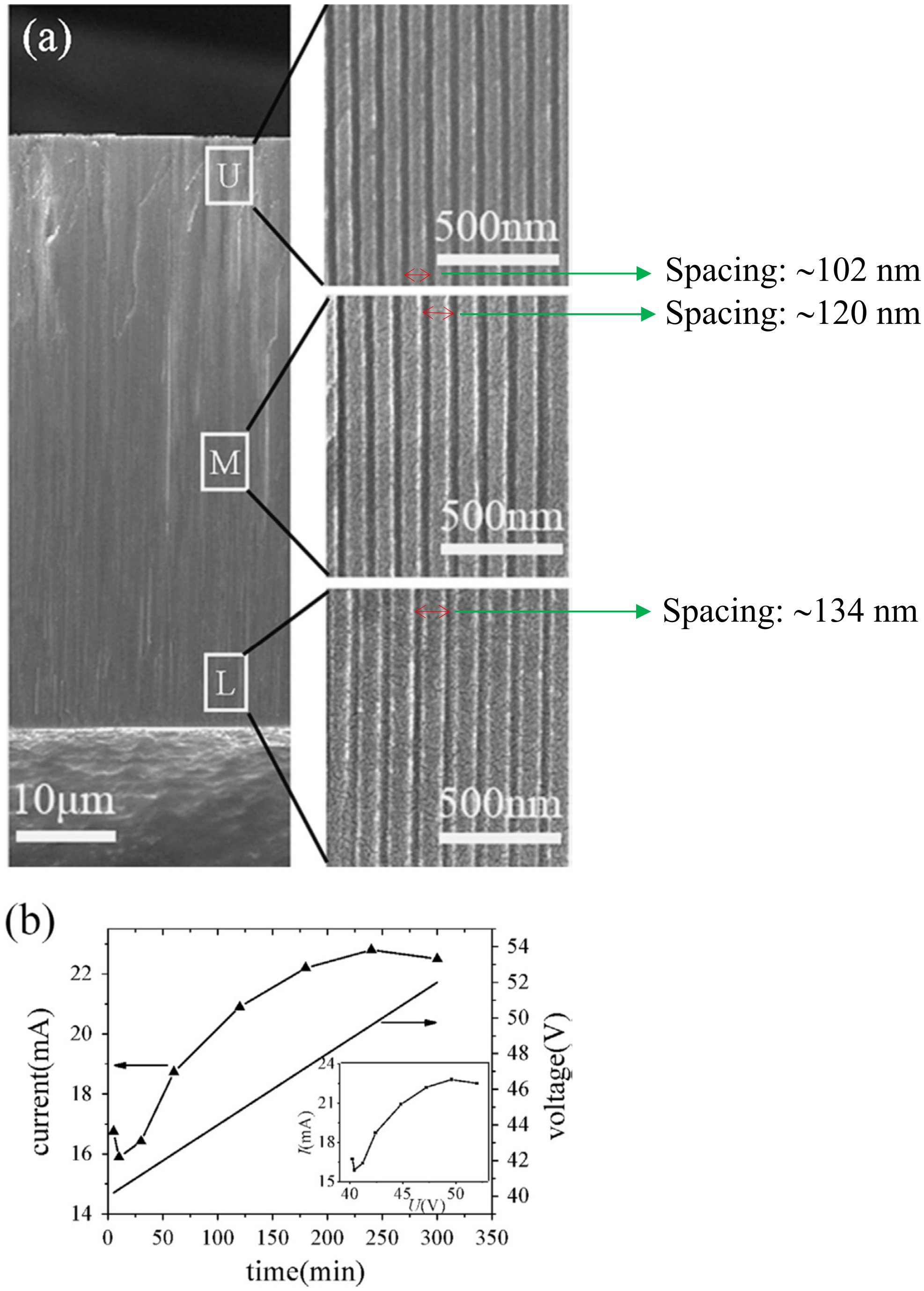

Fig. S13. (a) SEM images of sample with the compensation voltage increased from 40 to 52 V. (b) Current–time curve and applied voltage. Reproduced from G. L. Shang et al. *Mater. Lett.* **110**, 156-159 (2013).

On the other hand, although SEM images of the surfaces of AAO membranes fabricated under the voltage compensation mode were not given in the Shang's paper, we have supplemented the experimental data based on the voltage compensation method. Figs. S13(a1) and S13(a2) correspond to SEM images of the top and bottom surfaces of AAO membranes when the anodization voltage increases from 40 V to 52 V with a scan rate of 40 mV/min during the second anodization, it is clearly observed that the nanochannels on the top section (corresponding to the starting voltage of 40 V) basically keep the ordered arrangement, however, the ordered arrangement of the nanochannels on the bottom section (corresponding to the ending voltage of 52 V) has been damaged substantially (Fig. S14(a2)), especially, the majority of pores grown on the bottom surface are not regular as compared with those formed on the top surfaces, which further confirms that the whole nanochannels are not cylindrical. The supplemented experiments unambiguously testify that the uniform nanochannel diameter cannot be obtained by the voltage compensation method owing to breaking the self-ordering growth regime with the irregular shape of the nanochannels. Furthermore, to study the effect of voltage on the nanochannel structures, we have fabricated the AAO membranes by the voltage compensation from 40 V to 60 V. It is found the self-ordered arrangement of the nanochannels on the bottom surface has been damaged completely (Fig. S14(b2)), also most of the pores on the bottom surface present irregular shape.

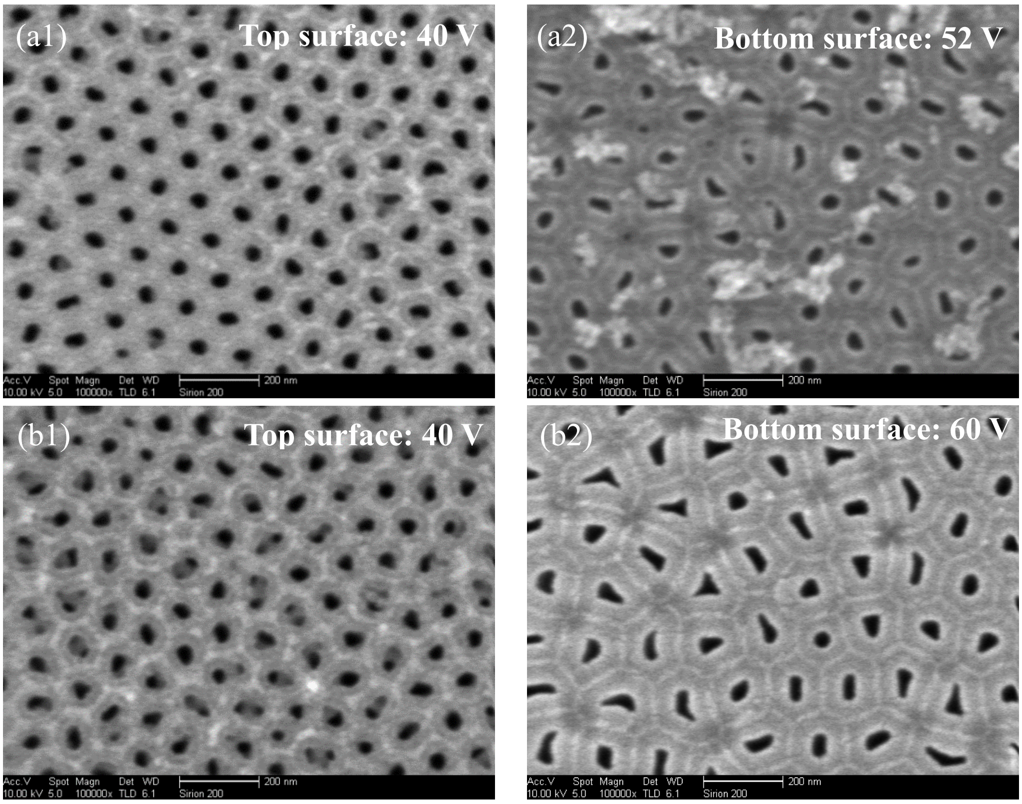

Fig. S14. SEM images of the AAO membranes fabricated by the voltage compensation method. (a1), (a2) Top and bottom surfaces for the voltage changing from 40 V to 52 V; (b1), (b2) Top and bottom surfaces for the voltage changing from 40 V to 60 V.

Secondly, in terms of our work, the AAO membranes were fabricated by the self-ordering regime with the constant voltage of 40 V.

Statistic measurements of 300 nanochannel spacings on the top and bottom surfaces in the AAO membrane formed by the self-ordering growth (Fig. S4), illustrate the average spacing is constant (102.5 nm). Figs. S15(a1) and S15(a2) display SEM images of the top and bottom surfaces of the as-prepared self-ordered AAO membrane (reproduced from Fig. S10). While Figs. S15(b1) and S15(b2) illustrate SEM images of the top and bottom surfaces of the same AAO membrane after the temperature gradient etching (reproduced from Fig. S10). It is observed the nanochannel size on the bottom surface (Fig. S15(a2)) is much smaller than that on the top surface (Fig. S15(a1)), but the spacing between adjacent nanocnanels on the bottom surface is the same as that on the top surface, indicating the growth orientation of the nanochannels is coaxial with upright nanochannels. After the temperature gradient etching, the nanochannel size on the bottom surface (Fig. S15(b2)) is equals to that on the top surface (Fig. S15(b1)), also the nanochannel spacings on both the bottom and top surfaces are constant after the etching. So, the cylindrical nanochannels can be achieved by the temperature gradient etching of the truncated conical nanochannels. also, the nanochannels fabricated by the self-ordering growth regime and subsequent temperature gradient etching, exhibit hexagonally self-ordered arrangement with regular nanochannels.

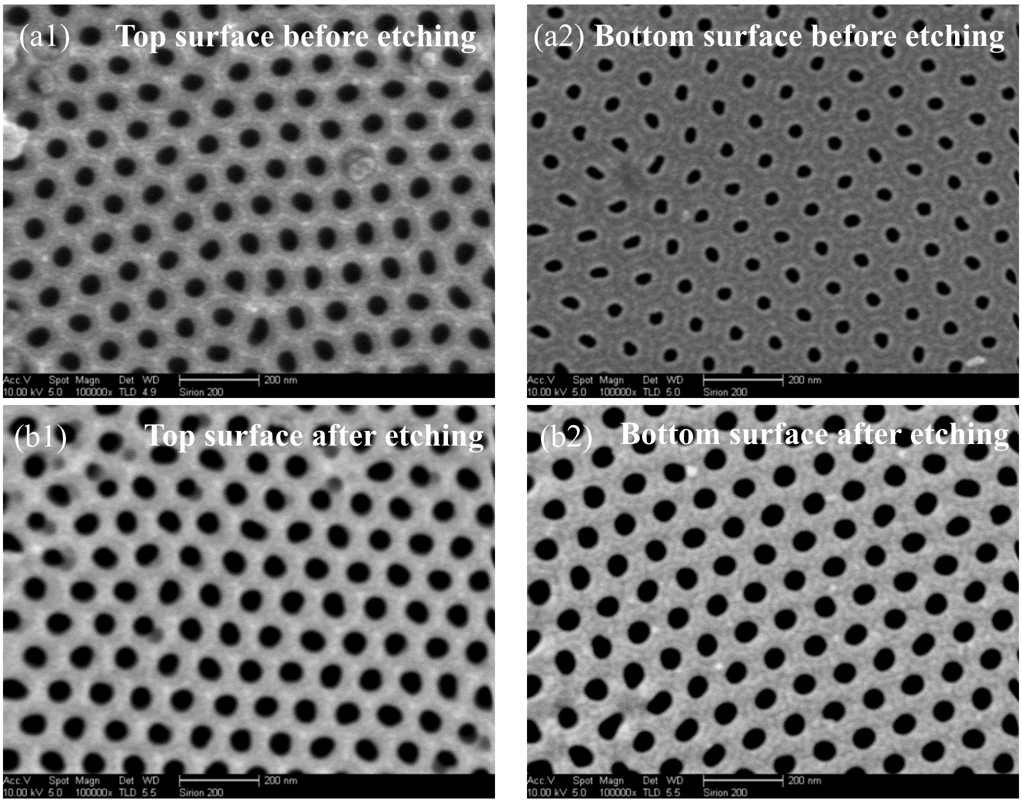

Fig. S15. SEM images of the AAO membrane fabricated by the self-ordering growth at the constant voltage of 40 V. (a1), (a2) Top and bottom surfaces of the as-prepared AAO membrane; (b1), (b2) Top and bottom surfaces via the temperature gradient etching.

The following table lists the comparisons of the nanochannels: one is the self-ordered AAO membranes fabricated by our constant anodization voltage method (self-ordering growth regime) and the subsequent temperature gradient etching, the other is the AAO membranes fabricated by the voltage compensation mode (non self-ordering growth regime) reported by Shang et al.

Comparison of parameters	**Self-ordering growth regime**	**Non self-ordering growth regime**
Anodization voltage	Constant (40 V)	Variable (increasing from 40 V to 52 V)
Spacing of nanochannels (D_{int})	**Constant** (102.5 nm)	**Variable** (from 102 nm to 134 nm)
Arrangement of nanochannels	**Self-ordered** nanochannel arrays	**Disordered** nanochannel arrays (on the bottom surface)
Growth orientation of nanochannels	**Coaxial** growth	**Non-coaxial** growth
Configurations of nanochannels	**High regular** shape (upright nanochannels) Truncated conical nanochannels in as-prepared AAO membranes **Cylindrical** nanochannels via the etching based on the temperature gradient regime	**Irregular** shape (winding nanochannels) **Non-cylindrical** nanochannels under the non-coaxial growth
Density of nanochannels	**Constant** ($1.1 \times 10^{10} cm^{-2}$) $\left(\frac{2}{\sqrt{3}D_{int}^{2}} \times 10^{14} cm^{-2}\right)$	**Variable** (cannot be calculated statistically due to the disordered arrangement of nanochannels)
References	Our work	Publication in Materials Letters 110 (2013) 156-159